Jonas Benzler,[1] Goutham K. Ganjam,[2] Dominik Pretz,[1] Rebecca Oelkrug,[1] Christiane E. Koch,[1] Karen Legler,[1] Sigrid Stöhr,[1] Carsten Culmsee,[2] Lynda M. Williams,[3] and Alexander Tups[1,4]

Central Inhibition of IKKβ/NF-κB Signaling Attenuates High-Fat Diet–Induced Obesity and Glucose Intolerance

Diabetes 2015;64:2015–2027 | DOI: 10.2337/db14-0093

Metabolic inflammation in the central nervous system might be causative for the development of overnutrition-induced metabolic syndrome and related disorders, such as obesity, leptin and insulin resistance, and type 2 diabetes. Here we investigated whether nutritive and genetic inhibition of the central IκB kinase β (IKKβ)/nuclear factor-κB (NF-κB) pathway in diet-induced obese (DIO) and leptin-deficient mice improves these metabolic impairments. A known prominent inhibitor of IKKβ/NF-κB signaling is the dietary flavonoid butein. We initially determined that oral, intraperitoneal, and intracerebroventricular administration of this flavonoid improved glucose tolerance and hypothalamic insulin signaling. The dose-dependent glucose-lowering capacity was profound regardless of whether obesity was caused by leptin deficiency or high-fat diet (HFD). To confirm the apparent central role of IKKβ/NF-κB signaling in the control of glucose and energy homeostasis, we genetically inhibited this pathway in neurons of the arcuate nucleus, one key center for control of energy homeostasis, via specific adeno-associated virus serotype 2–mediated overexpression of IκBα, which inhibits NF-κB nuclear translocation. This treatment attenuated HFD-induced body weight gain, body fat mass accumulation, increased energy expenditure, and reduced arcuate suppressor of cytokine signaling 3 expression, indicative for enhanced leptin signaling. These results reinforce a specific role of central proinflammatory IKKβ/NF-κB signaling in the development and potential treatment of DIO-induced comorbidities.

Obesity, as a consequence of overnutrition, reflects a high risk factor for the development of insulin resistance and ultimately type 2 diabetes (1,2). The hypothalamus represents a main insulin target tissue for regulating body weight and glucose metabolism (3–9). De Souza et al. (10) proposed that inflammatory alterations occur in the hypothalamus of rodents fed a high-fat diet (HFD). Subsequently, it has been established that diet-induced obesity (DIO) in rodents is associated with upregulation of proinflammatory pathways in the hypothalamus, involving activation of signaling intermediates such as c-Jun NH_2-terminal kinase (JNK) and IκB kinase β (IKKβ)/nuclear factor-κB (NF-κB) (10–14). In particular, Zhang et al. (14) established that the upregulation of the IKKβ/NF-κB pathway in the hypothalamus induced by an HFD was causative for the development of obesity. Specific activation of this pathway in the mediobasal hypothalamus aggravated some obesity parameters and impaired leptin and insulin signaling, whereas suppression of this pathway in the hypothalamus protected against DIO (14). Accumulating evidence suggests that HFD induces metabolic inflammation in the central nervous system, particularly in the hypothalamus, leading to the development of overnutrition-induced metabolic syndrome and related disorders such as obesity, leptin, and insulin resistance (10,13–17).

The IKKβ/NF-κB pathway, as a proinflammatory pathway, plays a pivotal role in classical immune response (18). In the unstimulated state, NF-κB remains in the cytoplasm in an inactive form and is bound to the inhibitory binding

[1]Department of Animal Physiology, Faculty of Biology, Philipps-University Marburg, Marburg, Germany
[2]Institute for Pharmacology and Clinical Pharmacy, Faculty of Pharmacy, Philipps-University Marburg, Marburg, Germany
[3]Metabolic Health Group, Rowett Institute of Nutrition and Health, University of Aberdeen, Aberdeen, U.K.
[4]Centre for Neuroendocrinology, Department of Physiology, School of Medical Sciences, University of Otago, Dunedin, New Zealand

Corresponding author: Alexander Tups, alexander.tups@otago.ac.nz.

Received 17 January 2014 and accepted 20 January 2015.

This article contains Supplementary Data online at http://diabetes.diabetesjournals.org/lookup/suppl/doi:10.2337/db14-0093/-/DC1.

protein IκBα. A broad range of immune stimuli can activate the upstream kinase IKKβ, leading to IκBα phosphorylation (at Ser^{32} and Ser^{36}) and degradation and subsequently to the release of NF-κB. Activated NF-κB enters the nucleus to induce transcription of target genes that mediate diverse cellular processes such as immunity, inflammation, proliferation, and apoptosis (19). Inhibition of IKKβ/NF-κB signaling in the mediobasal hypothalamus, via viral overexpression of IκBα, inhibited endoplasmic reticulum stress–induced glucose intolerance as well as systemic and hepatic insulin resistance (20). A recent study suggests that the hypothalamic transforming growth factor-β, which is excessively produced under conditions of obesity, accompanied by hyperglycemia and glucose intolerance, leads to accelerated mRNA decay of IκBα (21). These data suggest that anti-inflammation approaches may be beneficial in treating the impaired glucose tolerance caused by overnutrition. Secondary metabolites of herbs and spices are well known to act as antioxidants, to reduce proinflammatory cytokines, and to suppress inflammation (22) and are often used in traditional Chinese medicine. The flavonoid butein (3,4,2′,4′-tetrahydroxychalcone), which is found in plants such as *Caragana jubata* and *Rhus verniciflua*, inhibits NF-κB signaling by direct blockade of the upstream kinase IKKβ (23) and reduces adipocyte inflammation in vitro (24).

In the current study, we tested whether the IKKβ inhibitor butein could act in the brain to improve glucose or energy metabolism. For comparison, we examined whether adeno-associated virus serotype 2 (AAV2)–mediated inhibition of IKKβ/NF-κB signaling by overexpression of IκBα in the brain improves glucose and energy metabolism during obesity. Furthermore, the effects of IKKβ/NF-κB manipulation on hypothalamic insulin signaling and glucose and energy metabolism were explored. We first established that inhibition of IKKβ/NF-κB signaling via enteral or intracerebroventricular butein administration reveals potent glucose-lowering properties independent of whether obesity was caused by leptin deficiency or high-fat feeding. These effects were associated with improved insulin signaling involving the insulin receptor substrate (IRS) phosphatidylinositol 3-kinase (PI3K) pathway in the arcuate nucleus (ARC), one key brain region required for the control of glucose and energy homeostasis (5,25,26). In addition, the improved hypothalamic insulin signaling in response to chronic butein treatment was also reflected in beneficial effects on whole-body glucose homeostasis. To specifically inhibit downstream IKKβ/NF-κB signaling, an AAV2 construct allowing overexpression of IκBα was generated that was specifically injected into the parenchyma of the ARC. Moreover, the inhibitory serine phosphorylation sites of IκBα were replaced by alanine (IκBα mutant [IκBα-mt; serine 32 to alanine and serine 36 to alanine]), hindering nuclear translocation of NF-κB and therefore inhibiting downstream signaling events. Corroborating the essential role of central IKKβ/NF-κB signaling in the control of glucose and energy homeostasis, this treatment attenuated HFD-induced metabolic impairments.

RESEARCH DESIGN AND METHODS

Procedures involving animals were performed in accordance with national animal ethics legislation and received approval by the respective authorities for animal ethics. All experiments used male mice (C57BL/6J) and were purchased from Janvier (Le Genest-Saint-Isle, France). The animals were 7 weeks of age at the time of ARC-directed AAV2-IκBα-mt administration and housed individually under standard conditions with a light/dark cycle of 12 h. The ambient temperature for mice was 23°C. All animals had access to standard chow diet (cat. no. V1534, ssniff), low-fat diet (LFD), or HFD (containing 10 or 60% fat, respectively; cat. no. D12450B and D12492; Research Diets), as defined in the text, and water ad libitum. For central administration of drugs, cannulae were stereotaxically implanted into the left lateral ventricle as described previously (26).

Stereotaxic Injections

Intracerebral injections were performed under isoflurane anesthesia as described previously (26). Stereotaxic coordinates to reach the hypothalamic ARC are 1.5 mm posterior, ±0.3 mm lateral, and 6.1 mm ventral relative to bregma. AAV2 particles, containing 4×10^{10} vector genomes, were injected into the ARC using a 0.5 μL Hamilton glass syringe for 2 min. The injection needle remained in place at each injection site for an additional 5 min to allow for diffusion and prevent backflow. The incision was sutured and the animals were placed under a heating lamp to recover from the surgery.

Immunohistochemistry

In a first approach, we confirmed that butein inhibits hypothalamic IKKβ/NF-κB signaling in our experimental paradigm in vivo. Therefore, we analyzed the number of phospho-IκBα (Ser^{32}) immunoreactive cells after butein treatment relative to vehicle. Mice were fed an HFD for 3 weeks, fasted for 16 h, and divided into weight-matched groups. Butein was administered intracerebroventricularly (5 nmol in 1 μL artificial cerebral spinal fluid [aCSF]/5% DMSO) to one group of mice (n = 6), whereas the second group received an intracerebroventricular vehicle injection (aCSF/5% DMSO, n = 6) 30 min before terminal anesthesia and transcardial perfusion. Immunohistochemistry was carried out on mouse brain coronal cryosections as described previously (26,27), using an anti–phospho-IκBα (Ser^{32}) antibody (cat. no. 2859; Cell Signaling Technology).

To identify a possible interaction between butein and central insulin signaling, we investigated the phosphorylation of AKT in the ARC after butein treatment. Therefore, leptin-deficient ($Lep^{ob/ob}$) mice were fasted for 16 h and received intracerebroventricularly either butein (5 nmol in 1 μL aCSF/5% DMSO) or vehicle (1 μL aCSF/5% DMSO)

30 min before transcardial perfusion (n = 7/group). Immunohistochemistry was performed as described above, using an anti–phospho-AKT Ser^{473} antibody (cat. no. 4058; Cell Signaling Technology).

Glucose and Insulin Tolerance Tests

We analyzed whether the flavonoid butein (0.08, 0.8, or 8 mg/kg body weight in PBS containing 5% ethanol) is able to improve glucose tolerance. Therefore, 8-week-old Lep$^{ob/ob}$ mice were fasted for 16 h and received butein orally. Sixty minutes later, glucose (1.0 g/kg body weight) was intraperitoneally injected and a glucose tolerance test (GTT) was performed (n = 8/group). To determine the blood glucose levels, the vena facialis was repeatedly punctured and glucose concentrations were measured using a commercially available glucometer (Accu-Chek Performa; Roche). For statistical validation, the area under the curve (AUC) was calculated.

We next determined whether the effect of butein on glucose homeostasis was mediated via a central mechanism. Therefore, Lep$^{ob/ob}$ mice were fasted for 16 h and butein (5 nmol in 1 μL aCSF/5% DMSO) was intracerebroventricularly injected 30 min before glucose injection followed by an intraperitoneal GTT (IPGTT) as described above (n = 8/group). To assess whether potential effects of butein on glucose tolerance persist after chronic treatment, a group of Lep$^{ob/ob}$ mice received a daily intraperitoneal injection of butein (1 mg/kg body weight in PBS containing 5% ethanol) or vehicle (PBS containing 5% ethanol) for 7 days. During this time, food intake and body weight were monitored, and on the final day, an IPGTT was performed as described above (n = 10–11/group) (Supplementary Fig. 1).

We then investigated whether central administration of butein also improves glucose tolerance in DIO, glucose-intolerant mice. Mice were fed an HFD or respective LFD for 3 weeks, fasted for 16 h, and weight matched. Butein was administered intracerebroventricularly (5 nmol in 1 μL aCSF/5% DMSO) to one group of mice on HFD (n = 6), whereas the second group received an intracerebroventricular vehicle injection (aCSF/5% DMSO). The cohort on the LFD received vehicle intracerebroventricularly (aCSF/5% DMSO, n = 5–7/group) 30 min prior to the IPGTT.

We next determined whether the observed effects on glucose homeostasis were mediated via the IRS-PI3K pathway in the brain. To determine whether the antidiabetic properties of butein depend on intact insulin signaling in the brain, three groups of Lep$^{ob/ob}$ mice were fasted for 16 h and received two intracerebroventricular injections (1 μL each) 30 min apart. The first group received vehicle (5% DMSO/aCSF) followed by butein (5 nmol in 5% DMSO/aCSF). The second group received isoform-specific PI3K inhibitors (0.1 nmol in 5% DMSO/aCSF, PIK75/TGX221; both isoforms are required for insulin signaling in the CNS [27]) followed by butein (5 nmol in 5% DMSO/aCSF). The third group received two vehicle injections, and an IPGTT was performed as described above (n = 10/group).

We investigated whether overexpression of hypothalamic IκBα-mt might improve glucose tolerance. Therefore, after 5 weeks of HFD, mice were fasted for 16 h and received intraperitoneal glucose (1.5 g glucose/kg body weight), and an IPGTT was performed as described above. To determine whether IκBα-mt overexpression affects insulin sensitivity, an insulin tolerance test (ITT) was performed. After 7 weeks on HFD, mice were fasted for 16 h and received 27 USP units insulin/kg body weight intraperitoneally before the ITT was performed, and blood glucose values were analyzed as described above.

Recombinant AAV Vector Generation and Virus Production

The cDNA for IκBα-mt (serine 32 to alanine and serine 36 to alanine) was subcloned from the eukaryotic expression vector pBabe-GFP-IκB-α-mut (super repressor, 15264; Addgene) into an AAV2-hSyn-EGFP-WPRE (WHV [woodchuck hepatitis virus] posttranscriptional regulatory element) vector (28). IκBα-mt cDNA was amplified from the plasmid by PCR (phusion DNA polymerase) using the forward 5′-TTTAGCTAGCCCTCACTCCTTCTC-3′ and reverse 5′-CAGTGTACACCACTGTGCTGGC-3′ primers. These primers contain suitable *Nhe*1 and *Bsr*G1 restriction sites for cloning into the AAV construct. The amplified PCR product was first cloned into the pGemT easy cloning vector. The IκBα-mt cDNA fragment from the pGemT easy vector was subcloned into *Nhe*1 and *Bsr*G1 sites of AAV2-hSyn-EGFP-WPRE by replacing EGFP cDNA to obtain AAV2-hSyn-IκBα-mt-WPRE. In this vector system, the expression of IκBα-mt is under the control of the human synapsin-1 promoter to restrict the expression to neurons, and WPRE facilitates long-term expression of the transgene. All molecular cloning procedures were performed in SURE2 bacterial cells to minimize the recombination events. Virus transfection and production was performed as described previously (29). The ability of AAV2 vectors to drive neuronal expression of a transgene was validated by infecting differentiated Lund human mesencephalic (LUHMES) (human postmitotic dopaminergic neurons) cells ($P \leq 0.001$) (Supplementary Fig. 2*A* and *B*). Successful overexpression of IκBα-mt in the ARC was validated by in situ hybridization and revealed an 80% increase of IκBα expression in the ARC ($P \leq 0.001$) (Supplementary Fig. 2*C*).

Cell Culture

Differentiated LUHMES cells (30) were used to investigate the expression of neuronal-specific AAV2-hSyn-IκBα mutant virus. LUHMES cells were proliferated on flasks (Nunclon Delta surface) coated with 0.1 mg/mL poly-L-lysine (Sigma-Aldrich) overnight at 4°C. For the experiments, 0.6 million cells were seeded on six-well plates coated with 0.1 mg/mL poly-L-lysine overnight and washed three times with sterile water followed by coating with 5 μg/mL fibronectin (Sigma-Aldrich) overnight in the incubator (37°C, 5% CO_2). Twenty-four hours after plating, the medium was exchanged with differentiation medium (DMEM/F12 with

1% N2-supplement, 1 μg/mL tetracycline, 0.49 mg/mL dibutyryl cAMP [Sigma-Aldrich], and 2 ng/mL glial cell line–derived neurotrophic factor [R&D Systems]). Four days after differentiation, the medium was exchanged and infected with AAV2-EGFP as control and AAV2-hSyn-IκBα mutant viruses at a concentration of 10^{10} genomic units/mL. After 5 days of infection, the cells were lysed and the total protein was used to investigate the IκBα expression by Western blot.

Metabolic Measurement

We measured the effect of the AAV2-IκBα-mt on metabolic rate. Accordingly, carbon dioxide production and oxygen consumption were measured in metabolic cages (~5 L volume) that were connected to an open circuit respirometry system. Measurements were taken continuously for 24 h with a constant ambient temperature of 23°C. The airflow in the cage was adjusted to ~42 L/h and continuously monitored. The procedure has been described in detail previously (31).

In Situ Hybridization

To determine the mRNA expression of IκBα and suppressor of cytokine signaling 3 (SOCS-3) in the ARC, we performed in situ hybridization on coronal brain sections. As previously described (32), forebrain sections (16 μm) were collected throughout the extent of the ARC on to a set of 12 slides, with 12 sections mounted on each slide. Accordingly, the slides spanned the hypothalamic region approximating from −2.8 to −0.4 mm relative to bregma according to the atlas of the mouse brain (33). In situ hybridizations and analysis were performed as described previously (32).

Body Composition

To analyze body composition, mice were anesthetized with isoflurane (CP-Pharma) and were analyzed via DEXA scan (Lunar PIXImus Densitometer; GE Medical Systems).

Statistics

The data were analyzed by one-way ANOVA followed by a Holm-Šidák comparison test, as appropriate, using SigmaStat statistical software (Jandel). Where data failed equal variance or normality tests, they were analyzed by one-way ANOVA on ranks followed by Dunn multiple comparison test. The body weight data were analyzed by repeated-measures two-way ANOVA. The results are presented as means ± SEM, and differences were considered significant if $P \leq 0.05$.

RESULTS

The Flavonoid Butein Inhibits Central NF-κB Signaling and Improves Glucose Homeostasis

In the first experiment, we investigated whether butein inhibits IKKβ/NF-κB signaling in vivo. The potential of butein to inhibit IKKβ/NF-κB signaling is based on a direct interaction of butein with a cysteine residue in the activation loop of IKKβ (23) without affecting the phosphorylation status of the molecule. Therefore, we measured the number of phospho-IκBα (Ser^{32}) immunoreactive cells, the downstream target of IKKβ activity. A decrease in the number of phospho-IκBα immunoreactive cells would reflect inhibition of NF-κB signaling. Consistent with this interpretation, butein treatment decreased the number of phospho-IκBα (Ser^{32}) immunoreactive cells in the ARC by 40% compared with vehicle-treated mice ($P = 0.012$) (Fig. 1).

Hypothalamic NF-κB signaling is associated with obesity and the impairment of insulin and leptin signaling (13–17). As an initial approach, we tested whether nutritional inhibition of the IKKβ/NF-κB pathway by butein affects glucose homeostasis. Butein dose-dependently improved glucose tolerance in glucose-intolerant, $Lep^{ob/ob}$ mice as revealed by the IPGTT 60 min after oral administration. The two lower doses (0.08 mg/kg and 0.8 mg/kg) revealed a trend toward improved glucose tolerance compared with the vehicle-treated group, whereas the higher dose (8 mg/kg) significantly improved glucose tolerance in these mice relative to vehicle-treated controls ($n = 8$ animals/group, $P = 0.009$) (Fig. 2*A*). After this initial characterization, we sought to determine whether the effect of butein on glucose homeostasis was mediated through a central mechanism. Therefore, $Lep^{ob/ob}$ mice received intracerebroventricular butein (5 nmol) 30 min prior to glucose and an IPGTT was performed. Indeed, acute intracerebroventricular administration of butein also improved glucose tolerance in $Lep^{ob/ob}$ mice compared with the $Lep^{ob/ob}$ vehicle-treated group ($n = 8$/group, $P = 0.007$) (Fig. 2*B*).

Having established that butein acutely improved glucose tolerance, we investigated whether this effect persisted after chronic treatment. Daily intraperitoneal injections of butein (1 mg/kg body weight) for 7 days did not affect food intake or body weight (Supplementary Fig. 1). However, basal blood glucose levels (butein 147.9 ± 7.9 mg/dL vs.

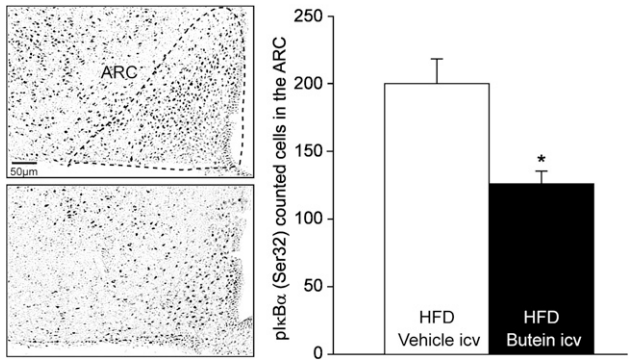

Figure 1—The chalcone butein inhibited central NF-κB signaling. Immunohistochemistry was performed on brain sections of wild-type mice fed an HFD. Butein (5 nmol in 5% DMSO in aCSF) or vehicle (5% DMSO in aCSF) was injected intracerebroventricularly (icv) 30 min before transcardial perfusion. The total number of phospho-IκBα (Ser^{32}) immunoreactive cells within the ARC was counted in four region-matched sections for each animal. Representative images of (Ser^{32}) immunoreactive cells in the ARC are shown. The dashed line indicates the area of the ARC, which was used to count the cells positive for IκBα. The bar graph shows the quantification of these cells. Results are means ± SEM. *$P \leq 0.05$. pIκBα, phospho-IκBα.

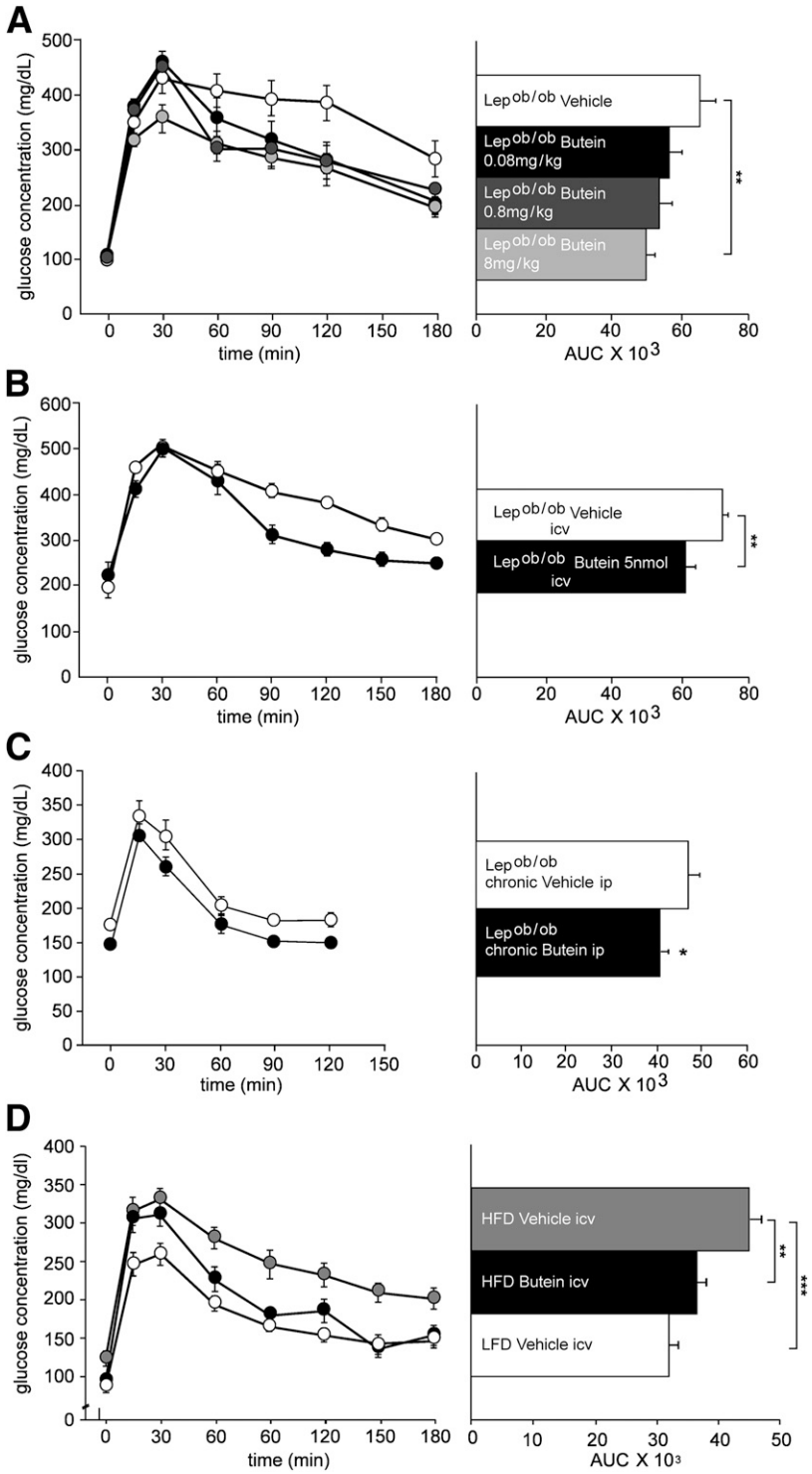

Figure 2—Butein improved glucose tolerance. *A*: Lep$^{ob/ob}$ mice received butein in three different concentrations (black circles, 0.08 mg/kg body weight in PBS/5% ethanol; dark gray circles, 0.8 mg/kg; light gray circles, 8 mg/kg) orally 1 h before an IPGTT was performed. Oral administration of butein dose-dependently improved glucose tolerance in Lep$^{ob/ob}$ compared with vehicle-treated mice (open circles, PBS/5% ethanol; n = 8/group). Shown are glucose concentrations (*left panel*) and associated AUC (*right panel*) during IPGTT. *B*: Intracerebroventricular (icv) injection of butein improved glucose tolerance in Lep$^{ob/ob}$ mice. IPGTT was performed 30 min after administration of butein (black circles, 5 nmol in 5% DMSO/aCSF) or vehicle (open circles, 5% DMSO in aCSF) into the lateral ventricle (n = 8/group). *C*: Chronic butein treatment improved glucose tolerance in Lep$^{ob/ob}$ mice. Mice received a daily intraperitoneal (ip) injection of butein (1 mg/kg body weight in PBS containing 5% ethanol) or vehicle (PBS containing 5% ethanol) for 7 days and an IPGTT (1 g glucose/kg body weight) was performed at day 7 (n = 10–11/group, P = 0.045). *D*: Butein was administered centrally to DIO mice before an IPGTT was performed using the protocol shown in *B*. The flavonoid improved glucose tolerance in wild-type mice fed an HFD for 3 weeks (black circles) relative to vehicle-treated controls (gray circles). This treatment improved glucose tolerance so profoundly that it was no longer different to mice on LFD (open circles, n = 5–7/group). Data show means ± SEM. *$P \leq 0.05$; **$P \leq 0.01$; ***$P \leq 0.001$.

vehicle 177.0 ± 6.0 mg/dL; $P = 0.014$) and glucose tolerance were significantly improved in mice that received chronic butein treatment relative to controls ($P = 0.045$) (Fig. 2*C*).

To verify that the glucose-lowering capacity of butein is not restricted to $Lep^{ob/ob}$ mice, we assessed its effect on glucose homeostasis in DIO mice. Intracerebroventricular injection of butein (5 nmol) 30 min prior to the IPGTT improved glucose tolerance significantly relative to the vehicle-treated group on the same diet ($P = 0.008$) so profoundly that no difference could be detected to the vehicle-treated cohort on the LFD group ($n = 5–7$/group) (Fig. 2*D*).

Since the above data suggest that butein acts at least in part through central mechanisms, we investigated whether the glucose-lowering properties of butein are mediated through interaction with hypothalamic insulin signaling. The number of cells positive for phospho-AKT (Ser^{473}) as a marker for PI3K activation (26) was strikingly increased in the ARC after central administration of butein (5 nmol in 1 μL aCSF/5% DMSO) by 66% relative to vehicle-treated (1 μL aCSF/5% DMSO) $Lep^{ob/ob}$ mice ($P = 0.003$, $n = 7$/group) (Fig. 3*A*).

To determine whether the central PI3K pathway is required for butein to display its antidiabetic properties, we determined whether the effect was blocked by pharmacological inhibition of PI3K. Intracerebroventricular injection of selective inhibitors of the PI3K catalytic subunits, p110α and p110β (PIK75 and TGX221) (27), in $Lep^{ob/ob}$ mice prior to intracerebroventricular butein application ($n = 10$) (Fig. 3*B*) fully blocked the ability of butein to improve glucose tolerance. The AUC of this group was identical to the group that received vehicle injections, whereas intracerebroventricular butein treatment without pretreatment with the PI3K inhibitors potently improved glucose tolerance (vehicle/butein vs. PI3K inhibitor/butein: $P = 0.019$; vehicle/butein vs. vehicle/vehicle: $P = 0.023$).

Overexpression of IκBα-mt Attenuates DIO

The ARC represents a key brain region for neuronal control of energy and glucose homeostasis. To test whether NF-κB–mediated inflammation in the ARC affects glucose and

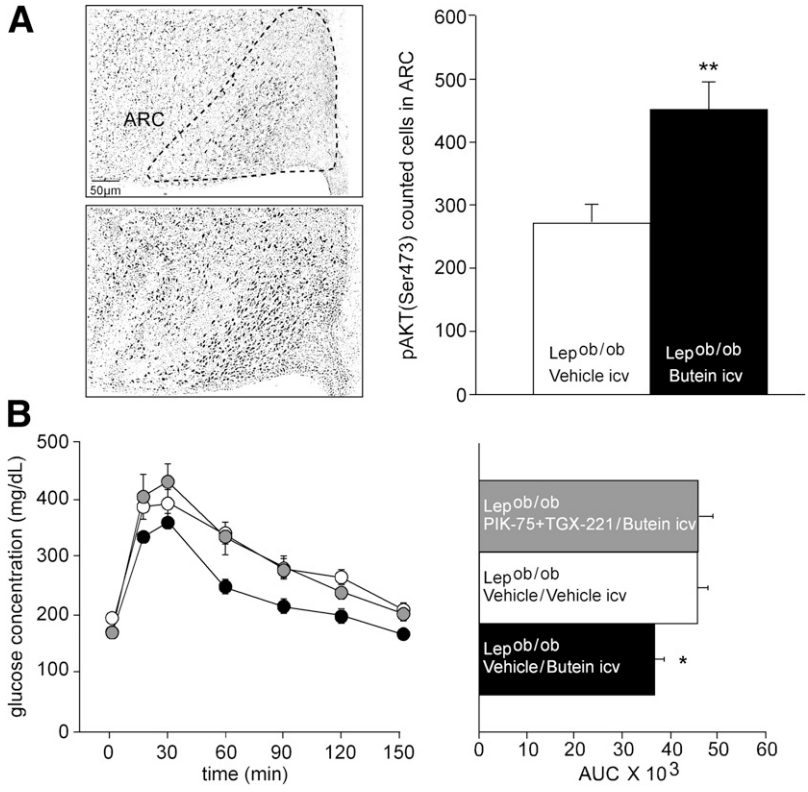

Figure 3—Butein and central insulin signaling. *A*: Intracerebroventricular (icv) administration of butein increased hypothalamic insulin signaling. Immunohistochemistry was performed on brain sections of $Lep^{ob/ob}$ mice after central administration of butein (5 nmol in 5% DMSO in aCSF) or vehicle (5% DMSO in aCSF) 30 min before transcardial perfusion. Inset depicts representative images of phospho-AKT (Ser^{473}) immunoreactive cells in the ARC. The bar graph shows the quantification of these cells. *B*: Central improvement of glucose homoeostasis by butein in $Lep^{ob/ob}$ mice was blocked by pretreatment with isoform-specific PI3K inhibitors (PIK75 and TGX221, each 0.1 nmol in 5% DMSO/aCSF), whereas butein alone improved glucose tolerance in these mice. The PI3K inhibitor was injected intracerebroventricularly 30 min before butein (5 nmol in 5% DMSO/aCSF), 30 min before the IPGTT (1.5 g glucose/kg body weight) was performed ($n = 10$ each group; vehicle/butein vs. PI3K inhibitor/butein: $P = 0.019$; vehicle/butein vs. vehicle/vehicle: $P = 0.023$). Shown are glucose concentrations (*left panel*) and associated AUC (*right panel*) during IPGTT. Results are means ± SEM. $^*P \leq 0.05$; $^{**}P \leq 0.01$. pAKT, phospho-AKT.

energy homeostasis, we inhibited NF-κB signaling via ARC-directed injection of 4×10^{10} genomic units of either AAV2-IκBα-mt (n = 6) or a control AAV2 virus (n = 10) into 8-week-old wild-type mice. Neuron-specific expression of IκBα-mt mRNA was facilitated by the human synapsin-1 promoter to restrict the expression to neurons. After 12 days on standard chow diet, both groups of mice did not differ in body weight and were switched to HFD for 50 days (Fig. 4*A*). Immediately after the shift to HFD, an elevation of the body weight trajectory occurred in both groups. However, the increase in body weight induced by the HFD was attenuated in AAV2-IκBα-mt mice compared with the mice that received the control virus. This effect became significant within 17 days after receiving the HFD and reached a plateau value of 10% less than the controls by day 38, which was sustained until the end of the study. DEXA analysis revealed a significant reduction of body fat mass (P = 0.027) (Fig. 4*B*) by ~35% of the AAV2-IκBα-mt group relative to the control cohort, whereas lean mass, bone mineral content (BMC),

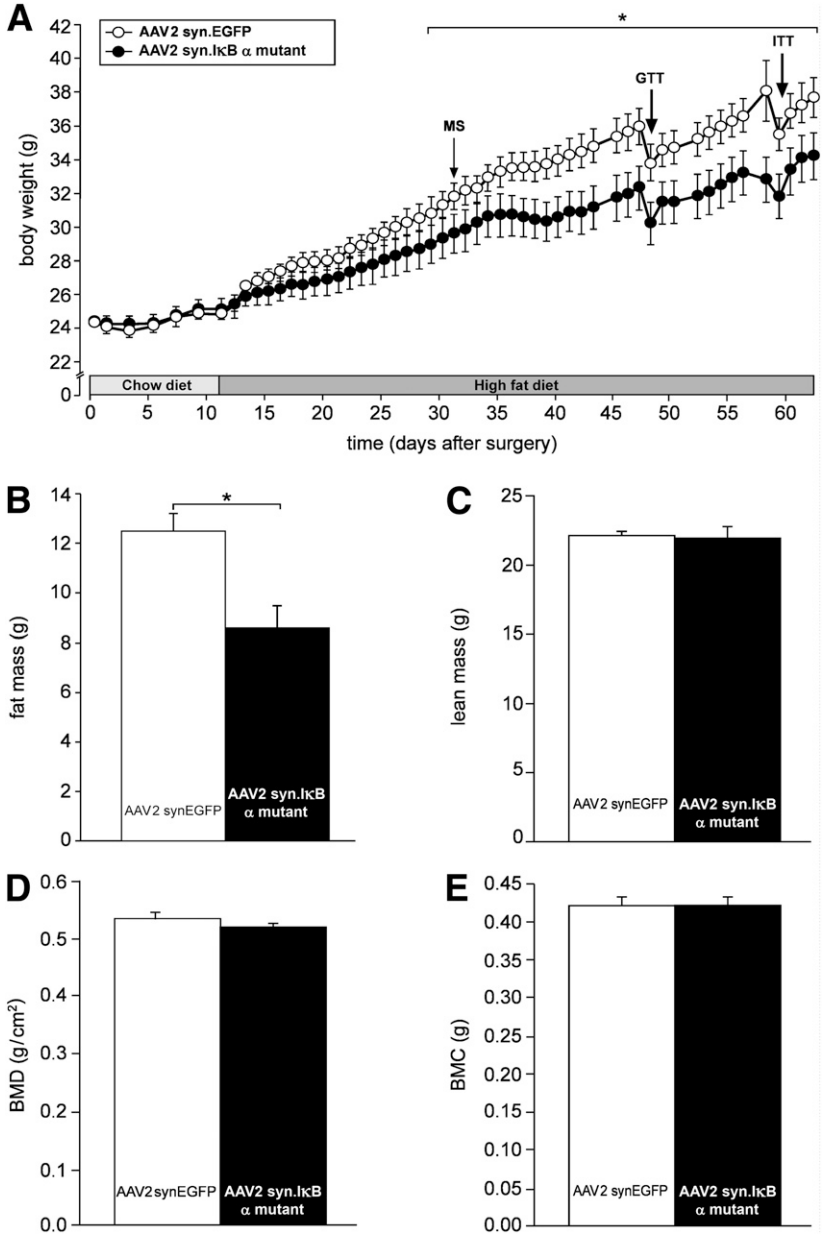

Figure 4—Neuron-specific AAV2-mediated overexpression of IκBα-mt in the ARC attenuated DIO. *A*: Wild-type mice were stereotaxically injected into the bilateral halves of the ARC with 2 × 250 nL of AAV2 virus expressing IκBα-mt (n = 6) or EGFP as a control (n = 10). Shown are the body weight trajectories of AAV2-EGFP and AAV2-IκBα-mt mice maintained on a chow diet (ad libitum) for 12 days followed by 50 days on an HFD (ad libitum). DEXA scan analysis revealed that body fat mass declined after treatment with AAV2-IκBα-mt virus on HFD (*B*), whereas lean mass (*C*), BMD (*D*), and BMC (*E*) did not change relative to AAV2-EGFP controls. MS, metabolic measurements. Results are means ± SEM. *$P \leq 0.05$.

and bone mineral density (BMD) were unaltered (Fig. 4*C*–*E*) by AAV overexpression of IκBα-mt in the ARC.

Overexpression of IκBα-mt Improves Glucose Homeostasis

Basal blood glucose levels were lower in the AAV2-IκBα-mt mice compared with the HFD controls ($P = 0.033$) (Fig. 5*A*). To determine whether NF-κB signaling in the ARC alters neuronal control of glucose homoeostasis, we performed an IPGTT in these mice on the 48th day after viral injection. Viral overexpression of IκBα-mt in the ARC improved glucose tolerance in comparison with the controls ($P = 0.011$) (Fig. 5*B*). Furthermore, the ITT revealed that the clearance rate of glucose was significantly increased in the AAV2-IκBα-mt mice relative to the AAV2-EGFP mice ($P = 0.027$) (Fig. 5*C*).

Metabolic Measurements

The mediobasal hypothalamus regulates energy balance by adjusting food intake to meet the metabolic needs of the animal (3,5–7,9). To explore whether ARC-directed IκBα overexpression alters metabolism, various metabolic markers were assessed. During the period of the metabolic measurements (day 33–34 after viral injection), no difference in food intake between AAV2-IκBα-mt (3.00 ± 0.2 g/24 h) and AAV2-EGFP mice (2.92 ± 0.09 g/24 h) could be detected (Fig. 6*A*). The food intake measurements were restricted to the period of metabolic

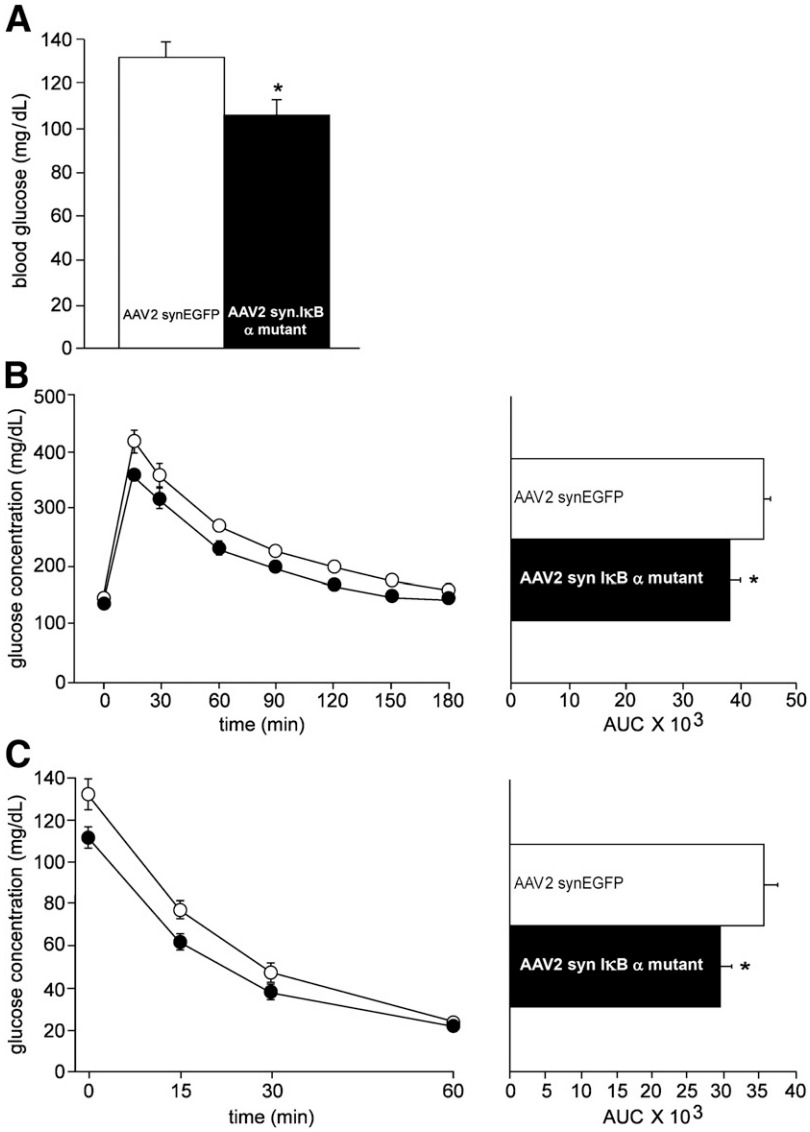

Figure 5—Overexpression of IκBα-mt in the ARC improved whole-body glucose homeostasis. *A*: Already after 46 days of HFD, mice overexpressing IκBα-mt exhibited decreased basal blood glucose levels relative to AAV2-EGFP controls. *B*: On day 48 on HFD, an IPGTT was performed and revealed improved glucose tolerance in AAV2-IκBα-mt mice compared with AAV2-EGFP mice. Mice overexpressing IκBα-mt exhibited enhanced insulin sensitivity as demonstrated by the ITT (*C*). Shown are glucose concentrations (*left panel*) and associated AUC (*right panel*) during IPGTT. Results are means ± SEM. *$P \leq 0.05$.

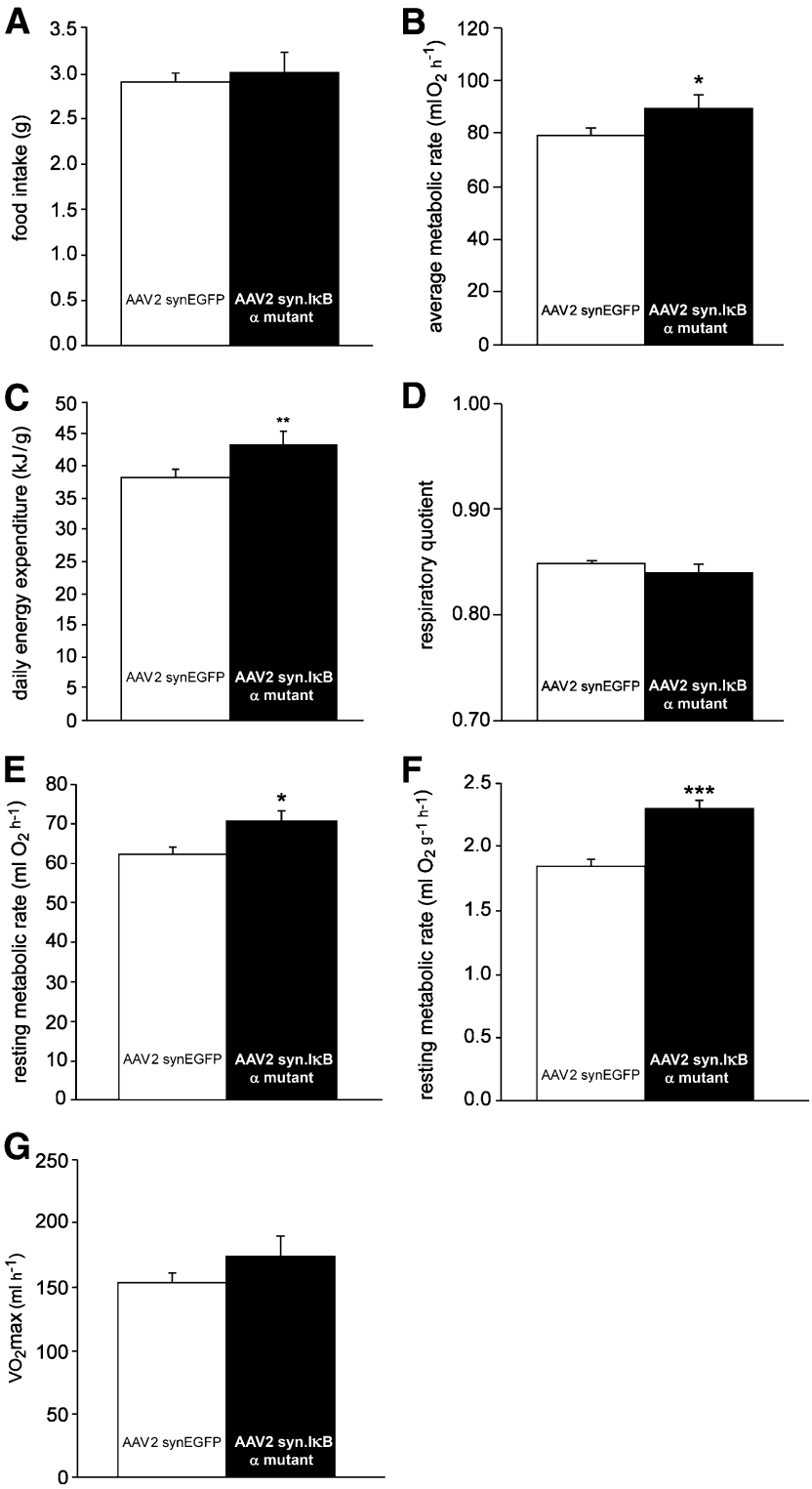

Figure 6—Metabolic measurements. After 3 weeks of HFD, the metabolic measurements revealed that food intake (*A*) was not affected. Average metabolic rate (*B*) and energy expenditure (*C*) were increased in the AAV2-IκBα-mt mice compared with the AAV2-EGFP mice, whereas respiratory quotient (*D*) was unaltered. Mice overexpressing IκBα-mt in the ARC showed elevated RMR (*E*) and RMR per gram body weight (*F*) compared with vehicle-treated mice, whereas maximal oxygen consumption (VO_2max) was not affected by this treatment (*G*). Results are means ± SEM. *$P \leq 0.05$; **$P \leq 0.01$; ***$P \leq 0.001$.

measurements due to the special caging system, which allowed accurate food intake measurement. High spillage rates seen in mice fed an HFD complicate longitudinal food intake measurements that require the long-term housing of mice in grid-bottomed cages, which can conflict with ethical concerns. However, average metabolic rate, measured as oxygen consumption, was increased by 13% in AAV2-IκBα-mt mice (90.2 ± 4.5 mL O_2 h^{-1}) relative to the AAV2-EGFP mice (79.5 ± 2.7 mL O_2 h^{-1}, $P = 0.049$) (Fig. 6*B*). Furthermore, daily energy expenditure in these mice was also elevated by 13% (43.3 ± 2.2 kJ/g) relative to AAV2-EGFP controls (38.2 ± 1.3 kJ/g, $P = 0.049$) (Fig. 6*C*), whereas the respiratory quotient was not different between the groups (AAV2-IκBα-mt 0.84 ± 0.008 vs. AAV2-EGFP 0.85 ± 0.002) (Fig. 6*D*). In addition, resting metabolic rate (RMR) was elevated in the AAV2-IκBα-mt group (70.5 ± 2.4 mL O_2 h^{-1}) relative to AAV2-EGFP controls (62.0 ± 2.1 mL O_2 h^{-1}, $P = 0.038$) (Fig. 6*E*), which corresponds to a 14% increase (Fig. 6*E*). A correction for the influence of body weight by calculating the RMR per gram body weight revealed an increase in RMR of 27% in AAV2-IκBα-mt mice (2.3 ± 0.07 mL O_2 g^{-1} h^{-1}) relative to the AAV2-EGFP controls (1.8 ± 0.06 mL O_2 g^{-1} h^{-1}, $P = 0.006$) (Fig. 6*F*). To exclude the possibility that the detected metabolic changes are not secondarily based on altered activity between the groups, the maximal oxygen consumption was assessed. Complying with unaltered activity, the maximal oxygen consumption did not differ between AAV2-IκBα-mt mice (173.8 ± 17.4 mL O_2 h^{-1}) relative to the AAV2-EGFP control mice (153.1 ± 8.8 mL O_2 h^{-1}) (Fig. 6*G*).

Arcuate Gene Expression of SOCS-3 Is Decreased in Response to ARC-Directed IκBα-mt Overexpression

To test whether ARC-directed AAV overexpression of IκBα-mt might alter leptin sensitivity on a molecular level, we investigated the expression of SOCS-3 as the most prominent inhibitor of leptin signaling (34,35). In situ hybridization analysis revealed that SOCS-3 mRNA was decreased by 35% in the ARC of AAV2-IκBα-mt mice relative to controls ($P = 0.029$) (Fig. 7).

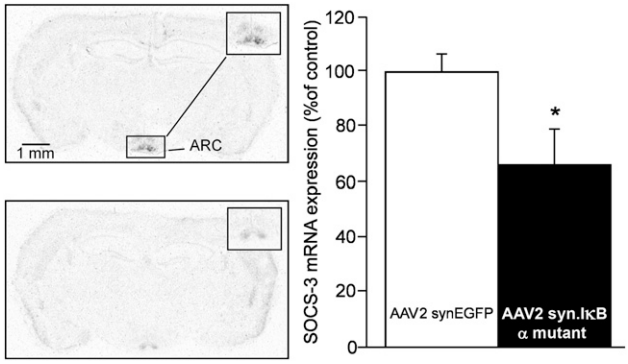

Figure 7—ARC-directed neuronal overexpression of IκBα-mt decreased SOCS-3 mRNA expression. IκBα-mt overexpression was associated with a decrease in SOCS-3 gene expression in the ARC. Representative autoradiographs of coronal brain sections exposed to a ^{35}S-labeled riboprobe against SOCS-3. Insets depict localization within the ARC of mice treated with AAV2-EGFP or AAV2-IκBα-mt. Semiquantitative analysis of gene expression of SOCS-3 in the ARC is presented in the bar graph as percentage of AAV2-EGFP. Results are means ± SEM. *$P \leq 0.05$.

DISCUSSION

Obesity and related metabolic disorders are largely the result of overconsumption of energy-dense foods, which are high in sugar and long-chain saturated fats. DIO leads to insulin resistance, with numerous studies showing that both obesity and insulin resistance are related to the presence of a low-grade inflammatory state (36). Some studies have shown that obesity is associated with inflammation in the hypothalamus (10–14), the central regulator of whole-body energy and glucose homeostasis (3–9). It appears that saturated fatty acids may directly activate toll-like receptor 4 (37), which subsequently leads to activation of the downstream JNK and IKKβ/NF-κB cascade (13,17,38). In particular, modulation of the IKKβ/NF-κB pathway at the level of IKKβ and the upstream adaptor regulatory protein MyD88 suggested that this cascade, once activated, induces diet-induced resistance to the adiposity signals leptin and insulin (14,16).

Although accumulating evidence supports the hypothalamic inflammation theory, studies combining the use of nutritive agents in a pharmacological way and a gene-therapeutic approach to functionally assess whether direct inhibition of this cascade leads to metabolic improvements are scarce. As an intervention strategy to combat experimental glucose intolerance in genetic and dietary mouse models of obesity, we identified the flavonoid butein as a potent glucose-lowering agent. The profound acute effects were also seen after chronic treatment. Butein treatment for 7 days led to a reduction in basal blood glucose levels and improved glucose tolerance relative to controls. The metabolic effect appears to be specific to glucose homeostasis since food intake and body weight were not affected by chronic butein treatment.

Dose-dependent enteral and intracerebroventricular application of butein profoundly improved glucose tolerance in $Lep^{ob/ob}$ mice, suggesting that the glucose-lowering effect of this substance is mediated via central signaling events. Indeed, within the ARC, where butein appeared to stabilize the protein IκBα, we identified activation of central insulin signaling as demonstrated by an increase in the number of cells positive for phospho-AKT (Ser^{473}), upon intracerebroventricular butein administration, which supports this hypothesis. In addition, the glucose-lowering properties of butein were completely blocked by central inhibition of the catalytic subunits p110α and p110β of PI3K, suggesting that this pathway is required for butein action in the brain. A related finding by Yu et al. (39) identified anti-inflammatory properties of tea saponins in the hypothalamus, supporting the idea that nutritive agents that reduce central inflammation can lead to improved metabolic function. The very potent

glucose-lowering potential of butein is supported by the finding that HFD-induced glucose intolerance was reversed after intracerebroventricular butein administration.

Since the anti-inflammatory properties of butein are mediated via inhibition of the IKKβ/NF-κB pathway (23), we tested the hypothesis that chronic gene-therapeutic inactivation of this cascade in neurons of the ARC might prevent HFD-induced metabolic derangements in mice. As a gene-therapeutic intervention, we overexpressed the regulatory molecule IκBα, which retains NF-κB in the cytoplasm. Constitutive binding of NF-κB to IκBα was facilitated by the generation of a mutant IκBα construct that cannot be phosphorylated by the upstream kinase IKKβ due to exchange of the inhibitory phosphorylation sites serine 32 and serine 36 to alanine. Potential adverse effects caused by viral-induced inflammation were circumvented by the use of AAV2, which does not cause adverse local immune responses in comparison with, for example, adenovirus (40,41). A study performed by Zhang et al. (14) has comprehensively assessed the role of the IKKβ/NF-κB pathway in the control of energy metabolism by elegantly combining central gene knockout and adenoviral manipulation of this pathway. The current study extends these data by specifically focusing on assessing the role of IκBα in metabolic control. Indeed, ARC-directed overexpression of IκBα-mt partially protected from HFD-induced weight gain, which was exclusively caused by a reduction in body fat mass, without changes in body lean mass, BMC, and BMD. The observed reduction in body weight gain in our study was similar to the body weight–lowering effect of an injection of the dominant-negative lentiviral vector into the mediobasal hypothalamus to inhibit IKKβ (14). Notably, parallel to the effects of butein, chronic inactivation of the NF-κB pathway in the ARC also improved glucose tolerance and additionally led to a reduction in basal blood glucose levels, confirming the therapeutic glucose-lowering potential of central IKKβ/NF-κB pathway inhibition. Although systemic low-grade inflammation involving the IKKβ/NF-κB cascade is also associated with high-fat feeding, blockade of this pathway exclusively in neurons of the ARC is sufficient to ameliorate HFD-induced glucose and insulin intolerance, confirming the central role of this brain region in regulating whole-body glucose homeostasis.

The metabolic measurements revealed no difference in food intake between the AAV2-IκBα-mt and AAV2-EGPF mice, as measured during metabolic monitoring. However, because food intake was only measured for a short period, we cannot exclude the possibility that the viral treatment influenced the total food intake profile of these mice over the longer time course of the treatment. We hypothesized, however, that the catabolic effect of IκBα-mt overexpression was assigned to an increase in energy expenditure. Indeed, average metabolic rate, measured as oxygen consumption, and energy expenditure were increased in the AAV2-IκBα-mt mice relative to the AAV2-EGPF mice. The respiratory quotient was unaltered between both groups, suggesting that the observed effects are not based on different substrate utilization. To distinguish whether the increased energy expenditure is due to an elevated basal energy requirement or altered physical activity, we measured RMR and maximal oxygen consumption. Whereas ARC-directed overexpression of IκBα-mt led to a marked increase in RMR, maximal oxygen consumption was unaltered, suggesting a selective elevation in basal energy requirement by blockade of the NF-κB pathway in the ARC, without changing physical activity. The ARC-directed IκBα-mt overexpression, which was restricted to neurons, led to the profound metabolic alterations. This suggests that neuronal inflammation, involving the IKKβ/NF-κB pathway, contributes to the development of DIO-induced metabolic syndrome. However, whether IKKβ/NF-κB signaling in different neuron populations, within the ARC, differentially alters glucose and energy metabolism remains to be identified in future studies.

Despite growing evidence that hypothalamic inflammation is involved in the pathogenesis of type 2 diabetes, the underlying mechanism of how local inflammation affects glucose metabolism is incompletely understood. An emerging role of the parasympathetic signals, delivered by the vagus nerve, has been suggested (42). Specifically, chronic endoplasmic reticulum stress that affects hypothalamic neuroendocrine pathways controlling energy metabolism has been suggested as a mediator of sympathetic disorders involved in conveying insulin resistance (20).

An important glucose-lowering hormone that sensitizes insulin action in the mediobasal hypothalamus is leptin (26,43–46). Some of the glucose-lowering effects of butein were similar to leptin. For instance, we recently showed that leptin exhibits a potent acute glucose-lowering capacity in $Lep^{ob/ob}$ mice, which was associated with increasing the number of pAKT immunoreactive cells in the ARC, thereby sensitizing insulin action (26). It is conceivable that diet-induced hypothalamic inflammation leads to relative leptin insensitivity, involving NF-κB–mediated transcription of the most prominent leptin inhibitor, SOCS-3 (34,35), which is a target gene regulated by this transcription factor (14). Inhibition of IKKβ/NF-κB signaling in the ARC was associated with a reduction of SOCS-3 expression in this nucleus. As SOCS-3 is a negative regulator of leptin signaling, these data are consistent with the hypothesis that leptin signal transduction will be enhanced. This, together with the fact that leptin increases energy expenditure and oxygen consumption (47), supports the speculation that the catabolic actions of this metabolic manipulation might be mediated by restoration of leptin sensitivity, despite ongoing high-fat feeding. Based on our previous data showing that enhanced leptin signaling in the hypothalamus leads to increased hypothalamic responses to insulin (26), we speculate that by restoring leptin signaling, ARC-directed overexpression of IκBα might enhance insulin sensitivity

in the hypothalamus and hence improve glucose tolerance (by the same mechanism induced by inhibition of IKKβ by butein). Future studies focusing on the possible restoration of leptin signaling by inhibition of hypothalamic inflammation and its consequence for reinstating insulin sensitivity are urgently required to provide evidence for this hypothesis.

Taken together, combining nutritive and gene-therapeutic inhibition of the central IKKβ/NF-κB pathway, our data strongly support the hypothalamic inflammation theory and might provide novel tools to combat HFD-induced metabolic disorders.

Acknowledgments. The authors thank William C. Hahn (Dana-Farber Cancer Institute, Boston, MA) for providing the pBabe-GFP-IκB-α-mut (super repressor) vector and David R. Grattan (University of Otago) for editorial suggestions.

Funding. This study was funded by the German Ministry of Education and Research (ref. no. 0315087) and the German Research Foundation (ref. no. 0315087 and 243471766 to A.T.). L.M.W. was funded by the Scottish Government's Rural and Environment Science and Analytical Services Division.

Duality of Interest. No potential conflicts of interest relevant to this article were reported.

Author Contributions. J.B. performed most of the experiments and wrote the manuscript together with A.T. G.K.G., D.P., R.O., C.E.K., K.L., and S.S. were involved in performing experiments and data analysis. C.C. provided LUHMES cells. L.M.W. contributed to editorial changes and data discussion. A.T. is the guarantor of this work and, as such, had full access to all the data in the study and takes responsibility for the integrity of the data and the accuracy of the data analysis.

References

1. Bastard JP, Maachi M, Lagathu C, et al. Recent advances in the relationship between obesity, inflammation, and insulin resistance. Eur Cytokine Netw 2006;17:4–12
2. Chan JC, Malik V, Jia W, et al. Diabetes in Asia: epidemiology, risk factors, and pathophysiology. JAMA 2009;301:2129–2140
3. Brüning JC, Gautam D, Burks DJ, et al. Role of brain insulin receptor in control of body weight and reproduction. Science 2000;289:2122–2125
4. Marks JL, Porte D Jr, Stahl WL, Baskin DG. Localization of insulin receptor mRNA in rat brain by in situ hybridization. Endocrinology 1990;127:3234–3236
5. Niswender KD, Morrison CD, Clegg DJ, et al. Insulin activation of phosphatidylinositol 3-kinase in the hypothalamic arcuate nucleus: a key mediator of insulin-induced anorexia. Diabetes 2003;52:227–231
6. Obici S, Zhang BB, Karkanias G, Rossetti L. Hypothalamic insulin signaling is required for inhibition of glucose production. Nat Med 2002;8:1376–1382
7. Obici S, Feng Z, Karkanias G, Baskin DG, Rossetti L. Decreasing hypothalamic insulin receptors causes hyperphagia and insulin resistance in rats. Nat Neurosci 2002;5:566–572
8. Okamoto H, Nakae J, Kitamura T, Park BC, Dragatsis I, Accili D. Transgenic rescue of insulin receptor-deficient mice. J Clin Invest 2004;114:214–223
9. Okamoto H, Obici S, Accili D, Rossetti L. Restoration of liver insulin signaling in Insr knockout mice fails to normalize hepatic insulin action. J Clin Invest 2005;115:1314–1322
10. De Souza CT, Araujo EP, Bordin S, et al. Consumption of a fat-rich diet activates a proinflammatory response and induces insulin resistance in the hypothalamus. Endocrinology 2005;146:4192–4199
11. Belgardt BF, Mauer J, Wunderlich FT, et al. Hypothalamic and pituitary c-Jun N-terminal kinase 1 signaling coordinately regulates glucose metabolism. Proc Natl Acad Sci U S A 2010;107:6028–6033
12. Benzler J, Ganjam GK, Legler K, et al. Acute inhibition of central c-Jun N-terminal kinase restores hypothalamic insulin signalling and alleviates glucose intolerance in diabetic mice. J Neuroendocrinol 2013;25:446–454
13. Posey KA, Clegg DJ, Printz RL, et al. Hypothalamic proinflammatory lipid accumulation, inflammation, and insulin resistance in rats fed a high-fat diet. Am J Physiol Endocrinol Metab 2009;296:E1003–E1012
14. Zhang X, Zhang G, Zhang H, Karin M, Bai H, Cai D. Hypothalamic IKKbeta/NF-kappaB and ER stress link overnutrition to energy imbalance and obesity. Cell 2008;135:61–73
15. Cai D. NFkappaB-mediated metabolic inflammation in peripheral tissues versus central nervous system. Cell Cycle 2009;8:2542–2548
16. Kleinridders A, Schenten D, Könner AC, et al. MyD88 signaling in the CNS is required for development of fatty acid-induced leptin resistance and diet-induced obesity. Cell Metab 2009;10:249–259
17. Thaler JP, Yi CX, Schur EA, et al. Obesity is associated with hypothalamic injury in rodents and humans. J Clin Invest 2012;122:153–162
18. Baeuerle PA, Baltimore D. NF-kappa B: ten years after. Cell 1996;87:13–20
19. Vaughan S, Jat PS. Deciphering the role of nuclear factor-κB in cellular senescence. Aging (Albany, NY Online) 2011;3:913–919
20. Purkayastha S, Zhang H, Zhang G, Ahmed Z, Wang Y, Cai D. Neural dysregulation of peripheral insulin action and blood pressure by brain endoplasmic reticulum stress. Proc Natl Acad Sci U S A 2011;108:2939–2944
21. Yan J, Zhang H, Yin Y, et al. Obesity- and aging-induced excess of central transforming growth factor-β potentiates diabetic development via an RNA stress response. Nat Med 2014;20:1001–1008
22. Chuang CC, McIntosh MK. Potential mechanisms by which polyphenol-rich grapes prevent obesity-mediated inflammation and metabolic diseases. Annu Rev Nutr 2011;31:155–176
23. Pandey MK, Sandur SK, Sung B, Sethi G, Kunnumakkara AB, Aggarwal BB. Butein, a tetrahydroxychalcone, inhibits nuclear factor (NF)-kappaB and NF-kappaB-regulated gene expression through direct inhibition of IkappaBalpha kinase beta on cysteine 179 residue. J Biol Chem 2007;282:17340–17350
24. Wang Z, Lee Y, Eun JS, Bae EJ. Inhibition of adipocyte inflammation and macrophage chemotaxis by butein. Eur J Pharmacol 2014;738:40–48
25. Gelling RW, Morton GJ, Morrison CD, et al. Insulin action in the brain contributes to glucose lowering during insulin treatment of diabetes. Cell Metab 2006;3:67–73
26. Koch C, Augustine RA, Steger J, et al. Leptin rapidly improves glucose homeostasis in obese mice by increasing hypothalamic insulin sensitivity. J Neurosci 2010;30:16180–16187
27. Tups A, Anderson GM, Rizwan M, et al. Both p110alpha and p110beta isoforms of phosphatidylinositol 3-OH-kinase are required for insulin signalling in the hypothalamus. J Neuroendocrinol 2010;22:534–542
28. Kügler S, Lingor P, Schöll U, Zolotukhin S, Bähr M. Differential transgene expression in brain cells in vivo and in vitro from AAV-2 vectors with small transcriptional control units. Virology 2003;311:89–95
29. Benzler J, Ganjam GK, Krüger M, et al. Hypothalamic glycogen synthase kinase 3β has a central role in the regulation of food intake and glucose metabolism. Biochem J 2012;447:175–184
30. Lotharius J, Falsig J, van Beek J, et al. Progressive degeneration of human mesencephalic neuron-derived cells triggered by dopamine-dependent oxidative stress is dependent on the mixed-lineage kinase pathway. J Neurosci 2005;25:6329–6342
31. Heldmaier G, Ruf T. Body temperature and metabolic rate during natural hypothermia in endotherms. J Comp Physiol B 1992;162:696–706
32. Mercer JG, Moar KM, Logie TJ, Findlay PA, Adam CL, Morgan PJ. Seasonally inappropriate body weight induced by food restriction: effect on hypothalamic gene expression in male Siberian hamsters. Endocrinology 2001;142:4173–4181
33. Paxinos G, Franklin K. *The Mouse Brain in Stereotaxic Coordinates. (2).* San Diego, CA, Academics, 2002
34. Bjørbaek C, Elmquist JK, Frantz JD, Shoelson SE, Flier JS. Identification of SOCS-3 as a potential mediator of central leptin resistance. Mol Cell 1998;1:619–625
35. Tups A, Ellis C, Moar KM, et al. Photoperiodic regulation of leptin sensitivity in the Siberian hamster, *Phodopus sungorus*, is reflected in arcuate nucleus

SOCS-3 (suppressor of cytokine signaling) gene expression. Endocrinology 2004; 145:1185–1193
36. Hotamisligil GS. Inflammation and metabolic disorders. Nature 2006;444: 860–867
37. Milanski M, Degasperi G, Coope A, et al. Saturated fatty acids produce an inflammatory response predominantly through the activation of TLR4 signaling in hypothalamus: implications for the pathogenesis of obesity. J Neurosci 2009;29:359–370
38. Thaler JP, Schwartz MW. Minireview: inflammation and obesity pathogenesis: the hypothalamus heats up. Endocrinology 2010;151:4109–4115
39. Yu Y, Wu Y, Szabo A, et al. Teasaponin reduces inflammation and central leptin resistance in diet-induced obese male mice. Endocrinology 2013;154: 3130–3140
40. Monahan PE, Samulski RJ. AAV vectors: is clinical success on the horizon? Gene Ther 2000;7:24–30
41. Wang J, Faust SM, Rabinowitz JE. The next step in gene delivery: molecular engineering of adeno-associated virus serotypes. J Mol Cell Cardiol 2011;50: 793–802
42. Milanski M, Arruda AP, Coope A, et al. Inhibition of hypothalamic inflammation reverses diet-induced insulin resistance in the liver. Diabetes 2012; 61:1455–1462
43. Kievit P, Howard JK, Badman MK, et al. Enhanced leptin sensitivity and improved glucose homeostasis in mice lacking suppressor of cytokine signaling-3 in POMC-expressing cells. Cell Metab 2006;4:123–132
44. Hill JW, Williams KW, Ye C, et al. Acute effects of leptin require PI3K signaling in hypothalamic proopiomelanocortin neurons in mice. J Clin Invest 2008; 118:1796–1805
45. German J, Kim F, Schwartz GJ, et al. Hypothalamic leptin signaling regulates hepatic insulin sensitivity via a neurocircuit involving the vagus nerve. Endocrinology 2009;150:4502–4511
46. Hedbacker K, Birsoy K, Wysocki RW, et al. Antidiabetic effects of IGFBP2, a leptin-regulated gene. Cell Metab 2010;11:11–22
47. Hwa JJ, Fawzi AB, Graziano MP, et al. Leptin increases energy expenditure and selectively promotes fat metabolism in ob/ob mice. Am J Physiol 1997;272: R1204–R1209